



# Study of the sneezing effects on the real human upper airway using fluid–structure interaction method

Hamidreza Mortazavy Beni<sup>1</sup> · Kamran Hassani<sup>1</sup> · Siamak Khorrammehr<sup>1</sup>

Received: 10 August 2018 / Accepted: 6 March 2019 / Published online: 19 March 2019  
© The Brazilian Society of Mechanical Sciences and Engineering 2019

## Abstract

Human pleural cavity pressure rises substantially because of Valsalva maneuver during sneezing. However, the deformations in the upper airway respiratory system significantly increase due to flow rate growth in sneezing, and laryngeal fracture can be mentioned as one of the symptoms of this severe deformation during the Valsalva maneuver. Therefore, the accurate study of the distribution of pressure and velocity, in this case, is very important. In the present study, using a real human upper airway model, the pressure and velocity of the air flow, generated in the tract during the sneezing, have been investigated. Moreover, using a spirometer device, the outlet flow rate from the mouth during the sneezing was obtained. The simulation results indicated that the inlet pressure to the tract, existing in the bronchus region, reached a maximum of 14 kPa. By having such pressure input, the highest deformation, created in the upper airway, was calculated using the fluid–structure interaction method and it has been confirmed that the majority of the deformation happened in the maxillary sinus as well as the thyroid cartilage.

**Keywords** Sneeze · Upper airway · Deformation · CFD · FSI

## 1 Introduction

Most previous studies on the upper respiratory system have been performed using computational fluid dynamics (CFD) method but actually, the respiratory system function should be considered as the interaction of air fluid and the walls of the system which is modeled by FSI technique. Because of Valsalva maneuver during sneezing, the pressure of the pleural fluid pressure is quite high. For example, when someone blows off the tight balloon, then his pleural cavity pressure is increased.

The sensitivity of the bronchi and trachea is like that very small amounts of foreign matter or any other cause of provocation result in the sneezing reflex. The larynx and especially the carina (where the trachea divides into two bronchi) are sensitive and the end bronchioles and even alveolus are susceptible to chemical stimulants such as chlorine

gas. While sneezing, first the vocal cords closed firmly and then, the abdominal muscles, exhalation muscles firmly are contracted, and the pressure rises. Finally, the epiglottis and the vocal cords suddenly are contracted and the air comes out extensively from the gap of the bronchi and trachea.

So far, extensive studies have been done on the mechanism and various aspects of the human respiration process. Zhang and Lessmann [1] studied the simulation of airflow and particle deposition through the diffusion process in a 3D model of human airway. They showed that both the inlet and outlet flow boundary conditions have significant effects on the flow. Cebra and Summers [2] studied the flow aerodynamics in the human bronchi and tracheal regions using the computational fluid dynamics. Decreased pressure and increased shear stress in the region of a stenosis were shown. Therefore, the correct selection of the outflow boundary condition in a real sneeze can have a significant impact on the region of a stenosis flow conditions as we also confirm and analyze in the current research.

Wen et al. [3] investigated the behavior of continuous and steady flow with a flow rate of 7.5 and 15 L per minute in the left and right cavities of the nose and compared it with numerical and experimental results. Martin and Finley [4] proposed a method based on the use of non-spherical

---

Technical Editor: Estevam Barbosa Las Casas, Ph. D.

✉ Kamran Hassani  
k.hasani@srbiau.ac.ir

<sup>1</sup> Department of Biomedical Engineering, Science and Research Branch, Islamic Azad University, Tehran, Iran

suspended particles and uniform magnetic field in the process of magnetic drug delivery. Unlike all the methods presented before, this method instead of relying on the application of magnetic force to particles in order to absorb them uses the magnetic moment to direct the particles in the desired direction. They tested this procedure for an experimental model of lung branch. Liu et al. [5] used CT scan images to model the flow in the bronchi branches and lung of a human. Moghadas et al. [6] studied the effect of nasal deviation on the air flow in the human upper airway. Nithiarasu et al. [7] examined the steady air flow in a realistic respiratory system. Tavakoli et al. [8] also studied the transfer and deposition of particles in micro-dimensions in the human upper airway respiratory system. In the above studies, most researchers have used numerical methods to investigate the normal flow of breathing in the upper respiratory system of human, while human respiratory reflux, such as sneezing, can greatly affect the quality of the results. Hence, in the current research, a numerical method for analyzing the functional state of sneezing has been developed.

Malve et al. [9] studied the unsteady turbulent air flow in the human trachea, considering the fluid–solid interaction during coughing. This group used ADINA and Mimics softwares for their study. They also used the airflow profile at the time of coughing as an input boundary condition. Recently, Chen et al. [10] have illustrated the exhalation air flow during coughing when a person covers the outlet of his or her mouth. They also numerically examined the effect of particle dispersion while coughing. According to the group's observations, covering the mouth when coughing can greatly reduce the velocity of particle dispersion. The results of two recent studies [9, 10] indicated that the effect of boundary condition of the wall, including the consideration of the boundary condition of fluid–solid interactions in the wall, can influence the outcome of cough reflex. In order to see the effect of the wall in sneezing reflexes, the problem was solved in a completely real condition using FSI method.

Many researchers have studied airflow velocity or mouth outlet during coughing. These values vary widely among different researchers and have been reported differently. According to Zhu et al. [11] calculations, the maximum airflow velocity exiting from mouth reaches 22 m/s during coughing. Tang and Settles [12], using image analysis method, achieved the velocity map during coughing. The group's observations indicated that the maximum velocity of the surrounding air reached 8 m/s. Gupta et al. [13] studied different people experimentally and concluded that the airflow rate exiting from mouth varied from 2 to 8 L per second in middle-aged people when coughing.

As mentioned above, although a number of researchers have studied the human respiratory system and the outlet flow rate during coughing, there is a lot of differences among the

results. This issue was much more complicated when other important phenomena called sneezing was discussed and less information was available. According to Wells [14], the outlet airflow velocity will reach 100 m/s during sneezing. Xhi et al. [15] estimated the velocity of large particles dispersed during sneezing about 50 m/s. According to Jennison and Edgerton [16] tests, the velocity of outlet particles during sneezing reaches 46 m/s. Tang et al. [17] reported the maximum velocity of outlet particles during sneezing as 4.5 m/s. Nishimura et al. [18] studied the process of sneezing using an image processing method with the help of a high-speed video recording system and estimated the initial velocity of the outlet particles more than 6 m/s.

Bourouiba et al. [19], with the numerical and experimental study of fluid dynamics during coughing and sneezing, concluded that outlet air flow in these two processes is turbulent. The amount of pressure generated by sneezing in the nasal area of a healthy person was measured by Gwaltney [20] and reported to be  $612 \pm 505$  Pascal. Recently, Rahiminejad et al. [21] simulated the sneezing process and modeled the effect of the closed nose or closed mouth of human upper airway on pressure and velocity distribution of air in the tract.

A few researchers have examined the effects of sneezing with closed human upper airway on human health. Faden et al. [22] showed the effect of this action which led to laryngeal fracture of an individual due to high pressure from the sneezing in this area. According to the reported results, this high pressure can also have other destructive effects. Martinez et al. [23] also reported a case of fracture of the thyroid cartilage and the pain caused by it in the neck region due to sneezing and high pressure caused by it. According to the group's results, closing both mouth and nose during sneezing was the main reason for these destructive effects.

Knowing that sneezing puts the most pressure on human upper airway, a clear understanding of pressure distribution, air flow velocity, and also the distribution of exhaled air from the tract during sneezing are more important issues. In this research, we tried to study the sneezing noting to experimental aspect and simulation of sneezing phenomena. For this purpose, the simulation of sneezing process was initially developed by preparing a 3D model of the respiratory system of a healthy 30-year-old male subject (Fig. 1). The boundary conditions were applied to the model where the data were extracted from an experimental study performed on the same person (Fig. 6).

## 2 Methods

In this study, a 3D model of the human upper airway was extracted from a 30-year-old male with Computer Tomography scan images. The geometry was digital medical images

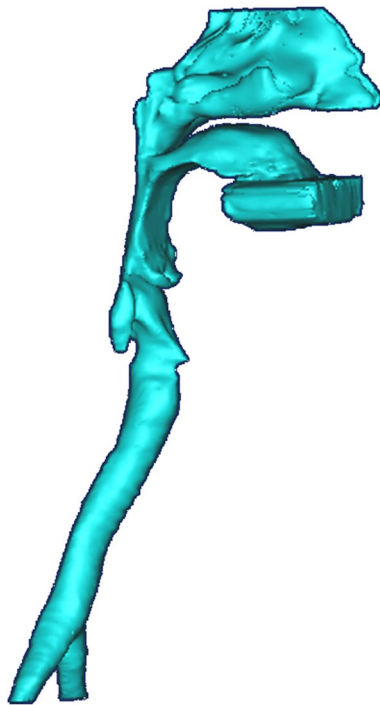


Fig. 1 Obtained geometrical model for numerical solution

in “Dicom” format which included 2D images. The first step was working on layers which had the optimal amount of upper and lower bounds of pixels for images. The geometry included nasal passages to the ends of the bronchi and air range. In fact, by adjusting this range, all areas of the air in the body could be identified and then, additional layers were deleted. After performing the necessary steps on a two-dimensional geometry, a three-dimensional model was formed and geometry was modified. As shown in Fig. 2, the considered geometry started from the nasal cavity and the oral cavity which ended in the trachea and ultimately bronchial tubes. Table 1 shows the different segments of the studied geometry.

To construct the airway model, CT scans of a 30-year-old male without any problems in his respiratory system were used in this study. The scans provided by TABA imaging center are obtained, while the person was in a supine status. Also to be more accurate, the mouthpiece of spirometer device had been put at the mouth in the time of imaging so that mouth is tight open like the sneezing test in the spirometer device. Under the professional supervision, the boundary between the airway mucosa and air in the upper respiratory tract was defined in each CT scans’ slices. To reconstruct, the 3D model consists of nasal cavity, pharynx, larynx, and trachea; the boundaries were imported to GAMBIT, a CFD preprocessor software. The boundaries are connected to each other to create a smooth surface and shape the volume. An unstructured triangular hybrid volume

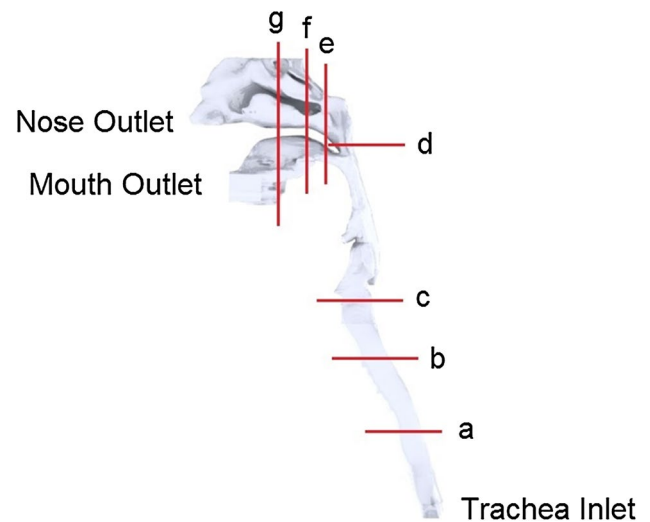


Fig. 2 Different sections in the computational model

mesh was generated inside the airway passage. A grid size of approximately 2,600,000 cells was obtained after the grid independency test.

The CFD package, fluent 6.3(ANSYS, USA), was utilized to solve the governing equations for the air flow in the complicated geometry of the human upper airway. Two conditions were considered in the present work. In the first case, the inlet pressure of the bronchial tubes was considered to be 2.8 kPa. In the second case, this pressure was raised to 14 kPa and that zero pressure was established in the outlet. No-slip condition (wall) was assumed on the mouth outlet for sneeze with closed mouth. A FSI boundary was defined at the inner surface of the upper airway wall (see Sect. 3).

Hybrid mesh has been used for the studied geometry (Fig. 3). In order to study the flow adjacent to the wall regions more accurately, prismatic elements were generated. In other regions of the studied geometry, triangular and tetrahedral elements were chosen. The grid contained six million elements, including seven thousand prism elements. It should be noted that the number of elements has

Table 1 Size of the cross sections considered in the computational model

Cross section	Area (cm <sup>2</sup> )
Bronchus	2.31
a	2.48
b	2.62
c	2.68
d	3.24
e	9.05
f	7.24
g	9.93
Mouth outlet	9.22
Nose outlet	2.73

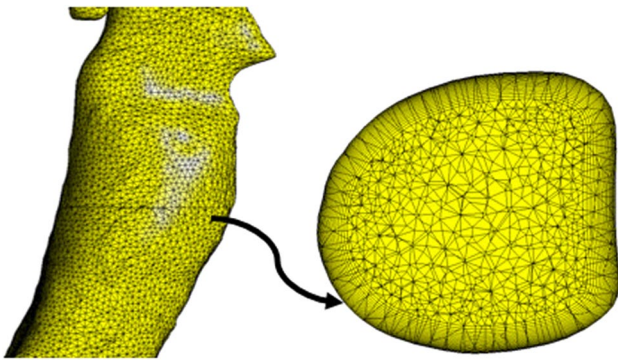


Fig. 3 Prismatic boundary layer grids adjacent to the wall

Table 2 Grid characteristics on respiratory system

Total grid number	2,683,478
Total element number	6,301,363
Prismatic elements	1,580,039
Trihedral elements	4,713,908
Tetrahedral elements	7416

been obtained after grid sensitivity study. The maximum  $y^+$  adjacent to the geometry wall was five which led to high accurate computations adjacent to the wall. The grid characteristics are shown in Table 2.

In order to estimate the height of the first layer of grids adjacent to the wall, which is very effective on the accuracy of the solutions, the following configuration was used (Fig. 4). The thickness of the first sub-layer of the

boundary layer on internal areas of the respiratory system was 0.028 mm, and the total number of layers was 20 layers at a growth rate of 1.1. In fact, the thickness of the entire boundary layer was considered to be 1.6 mm for numerical solution. A schematic of the grid generated in some sections of the geometry is shown in Fig. 5.

In the present study, as one of the noticeable performed simulations in the field of sneezing, the process was considered quasi-steady. The fluid was considered to be air with a density of  $1.225 \text{ kg/m}^3$ . The wall of the examined geometry was assumed to be rigid. According to what was reported by Rahiminejad et al. [21], Mylavarapu et al. [24], and Zubair et al. [25], the best way for simulating turbulent flows in complex geometries, such as the geometry studied in this study, is to adopt the SST-kw (Shear Stress Transport kw) method. Therefore, this method was used to solve the flow field in the complex respiratory system with computational fluid dynamics method. The flow regime was considered turbulent and incompressible. Also, due to the low fluid pressure drop along the path, the air density was considered constant in this numerical simulation.

As already mentioned, the outcomes of the experimental study have been used as a boundary condition in numerical simulation. For this purpose, a spirometer device was used in order to measure the outlet flow rate from the mouth during sneezing. It should be noted that the CT scan images, which were used in the numerical simulation, belonged to the same person. The case was a healthy non-smoking 30-year-old male without any respiratory disease and CT scan images were taken from him. Using spirometer device, the amount of the outlet flow rates during sneezing were obtained experimentally.

Fig. 4 Estimation of the height of the first sub-layer of flow solution mesh in the wall

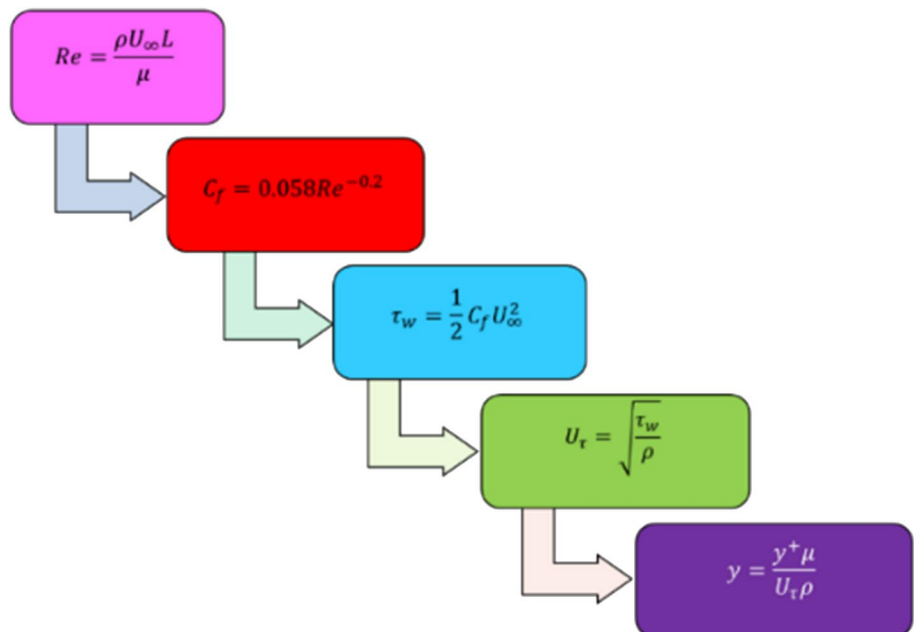
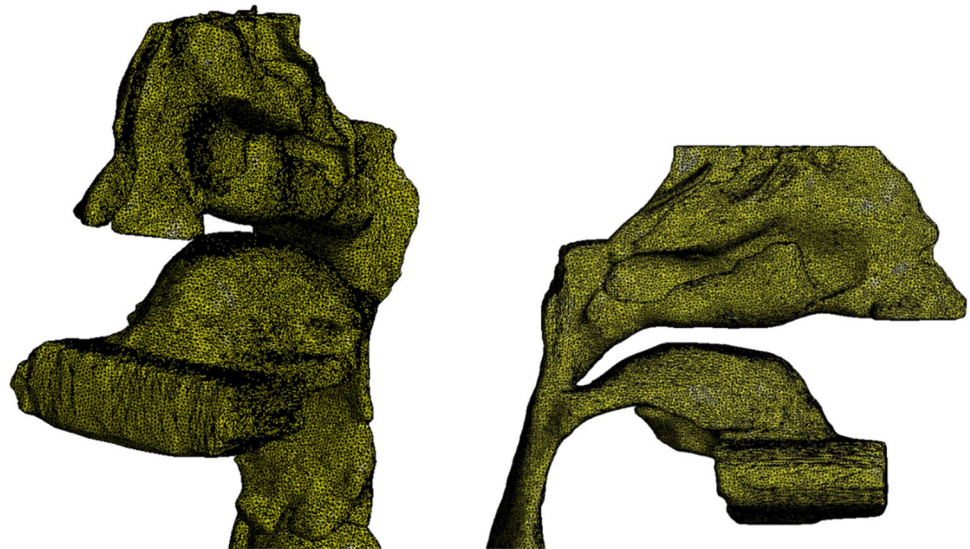


**Fig. 5** Generated grids on the human respiratory system from side view and isometric view



Accordingly, the data were collected by inserting the mouthpiece well into the mouth beyond the teeth to be carefully ensured that air cannot escape from the sides of the mouth. The data were retrieved from MiniSpir™ [26] during the tests, which were sent to the PC in digital form and managed by the WinspiroPro software. Before using the spirometer device, a calibrated 3-L syringe was used to calibrate the device. It should be noted that the spirometer is calibrated when the air is injected 3 L to the machine, the error rate is not greater than 3% or 90 mL. In other words, the number recorded by the device should be between 2.91 and 3.09 L.

### 3 Governing equations and boundary conditions

Based on Zhao et al. [27] study, the estimated range of Reynolds numbers (Re) indicated that the upper airway flow was laminar or transitional in sleep apnea. According to the reported results by Malve et al. [9], air flow in the human trachea was turbulent during coughing considering the fluid–solid interaction. The standard *k*– $\omega$  shear stress transport (*k*– $\omega$  SST) model was proven to be appropriate for simulating this complex flow. The main governing equations of the fluid domain can be expressed as:

$$\frac{\partial u_i}{\partial x_i} = 0 \tag{1}$$

$$\rho u_i \frac{\partial u_j}{\partial x_i} = -\frac{\partial p}{\partial x_i} + \frac{\partial}{\partial x_i} \left[ \mu \left( \frac{\partial u_i}{\partial x_j} + \frac{\partial u_j}{\partial x_i} \right) - \overline{\rho u'_i u'_j} \right] \tag{2}$$

where *u* is the fluid velocity,  $\rho$  is the fluid density, *P* is the fluid pressure,  $\mu$  is the dynamic viscosity, *i* and *j* represent the Cartesian coordinates. The fluid and solid domains were

coupled through the stress tensor. The Cauchy stress tensor in an isotropic Newtonian fluid field was:

$$\sigma_{ij}^f = -p\delta_{ij} + 2\mu \left( \epsilon_{ij} - \frac{1}{3}\epsilon_{kk}\delta_{ij} \right) \tag{3}$$

where  $\sigma_{ij}^f$  is the fluid stress tensor,  $\delta_{ij}$  is Kronecker delta, and  $\epsilon_{ij}$  is the rate of the strain tensor which is given by:

$$\epsilon_{ij} = \frac{1}{2} \left( \frac{\partial u_i}{\partial x_j} + \frac{\partial u_j}{\partial x_i} \right) \tag{4}$$

In the structural field, the governing equation of linear elasticity is:

$$\frac{\partial \sigma_{ij}^s}{\partial x_j} + F_i = \rho \frac{\partial^2 D_i}{\partial t^2} \tag{5}$$

where  $F_i$  is the body forces,  $D_i$  is the structural displacement,  $\sigma_{ij}^s$  is the solid stress tensor, *t* is the time. The Cauchy stress tensor in the structural field is defined as:

$$\sigma_{ij}^s = \frac{Ev}{(1+\nu)(1-2\nu)} \epsilon_{kk}\delta_{ij} + \frac{E}{(1+\nu)} \epsilon_{ij} \tag{6}$$

where *E* is Young’s modulus,  $\nu$  is the Poisson’s ratio,  $\epsilon_{ij}$  is the strain tensor Eq. (4). The coupling conditions of fluid and solid domain at the FSI boundary are the matching of the fluid velocity and structural displacement:

$$u_i = \frac{\partial D_i}{\partial t} \tag{7}$$

and the force equilibrium across the FSI interface:

$$\sigma_{ij}^f n = -\sigma_{ij}^s n \tag{8}$$

where  $n$  is the normal vector outward of the FSI interface. The coupling conditions of fluid and solid domains, at the FSI boundary, are the matching of the fluid velocity and structural displacement:

$$u_i = \frac{\partial D_i}{\partial t} \quad (9)$$

and the force equilibrium across the FSI interface:

$$\sigma_{ij}^f n = -\sigma_{ij}^s n \quad (10)$$

where  $n$  is the normal vector outward of the FSI interface. A uniform Poisson ratio of  $\nu = 0.33$  and an isotropic Young's modulus of 1000 Pa were used for the soft palate. This is based on Birch et al. [28] who reported ex vivo measurements of the soft palate having a Poisson ratio range between  $\nu = 0.3 - 0.45$  and a Young's modulus distribution with a mean of 585 Pa at regions near the uvula to 1409 Pa near attachment regions. The fluid was considered to be air with a density of  $1.225 \text{ kg/m}^3$  and dynamic viscosity of  $\mu = 1.795E - 05 \text{ (N.s/m}^2\text{)}$ .

In the present work, the governing equations were converted to the algebraic equations to solve the flow field and use the control volume method. In order to couple the velocity and pressure equations, the SIMPLE algorithm [29] was used. The inlet boundary condition in the bronchi region was considered as the pressure inlet. The nasal and mouth outlets were open and the pressure outlet boundary condition (gauge pressure is zero) was set at these regions. No-slip boundary condition was considered in the walls of the system.

Using the obtained data from the spirometer, a specific air-flow rate (derived from the experimental study) was used as an inlet air flow in the bronchial area. Figure 6 shows the flow rates from the mouth outlet during sneezing.

According to the figure, the flow rate reached to more than 10 L/s during sneezing. For the studied case, the outlet flow rate was measured three times and the mean maximum and average flow rates were obtained as 10.58 L/s and 4.79 L/s, respectively.

In fact, having an outlet flow rate from the mouth of the individual during sneezing along with a trial and error solution, the inlet pressure in the bronchial region was adjusted. The adjustment was based on how the simulated outlet flow rate coincides with the outlet flow rate measured by the spirometer. Therefore, two pressures, equal to 14 and 2.8 kPa, were set as the inlet boundary condition to extract the maximum and average flow rate from the mouth, respectively.

## 4 Results

As mentioned in the previous section, the inlet pressure of the bronchial tubes was considered to be 14 kPa to reach the maximum flow rate of the mouth outlet (10.58 L/s).

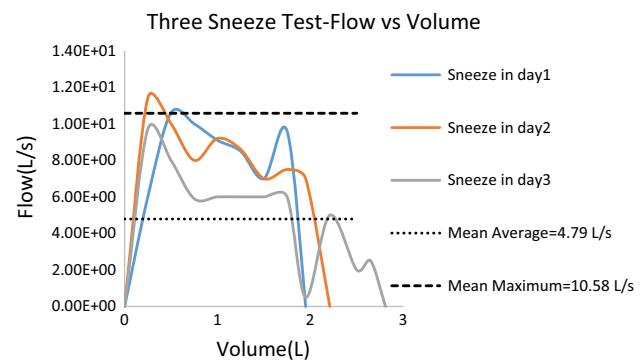


**Fig. 6** Experimental measured flow rates from mouth outlet while sneezing

Also, the results of speed and pressure in shapes and charts in seven sections (a, b, c, d, e, f, g) are given in Fig. 2.

As mentioned in the previous section, two conditions were considered in the present work. In the first case, the inlet pressure of the bronchial tubes was considered to be 2.8 kPa in order to reach the measured flow rate equivalent to the average flow rate of mouth outlet (4.79 L/s). In the second case, this pressure was increased to 14 kPa to reach the maximum flow rate of the mouth outlet (10.58 L/s). In the following, the results of these two cases are presented. Also, the results of speed and pressure in shapes and charts in seven sections (a, b, c, d, e, f, g) are given in Fig. 2.

*Case 1* Bronchus Inlet pressure of 2.8 kPa

The maximum speed and static pressure values at different sections in case 1 are shown in Fig. 7. As it is illustrated in Fig. 7, considering different sections in the domain, the maximum speed occurred in section d. Hence, the particles which leave the respiratory system during sneezing will diffuse with significant velocities.

The results of the inlet and outlet flow rates for normal sneeze (case 1) are shown in Table 3. The results reveal that the outlet flow rate of nose is 2.3 L/s. Comparing this flow rate with outlet flow rate of the mouth, it was observed that about 32% of the outlet flow rate during sneezing exited from the nose and the rest (68%) exited from the mouth. Therefore, it can be concluded that the total average flow rate, in this case, was 7.23 L/s, which occurred at the inlet of the bronchus. The flow velocity of the nose outlet was about 2.2 times greater than the mouth outlet.

The average velocity and static pressure values at different sections for case 1 are shown in Fig. 8. According to Fig. 8, the highest average pressure has occurred in the trachea. The maximum average velocity was at section A, which also is in trachea.

*Case 2* Bronchus Inlet pressure of 14 kPa

The maximum static pressure and velocity on each section for the case 2 are shown in Fig. 9. In this case, the

**Fig. 7** Maximum speed and static pressure values at different sections for normal sneeze (case 1)

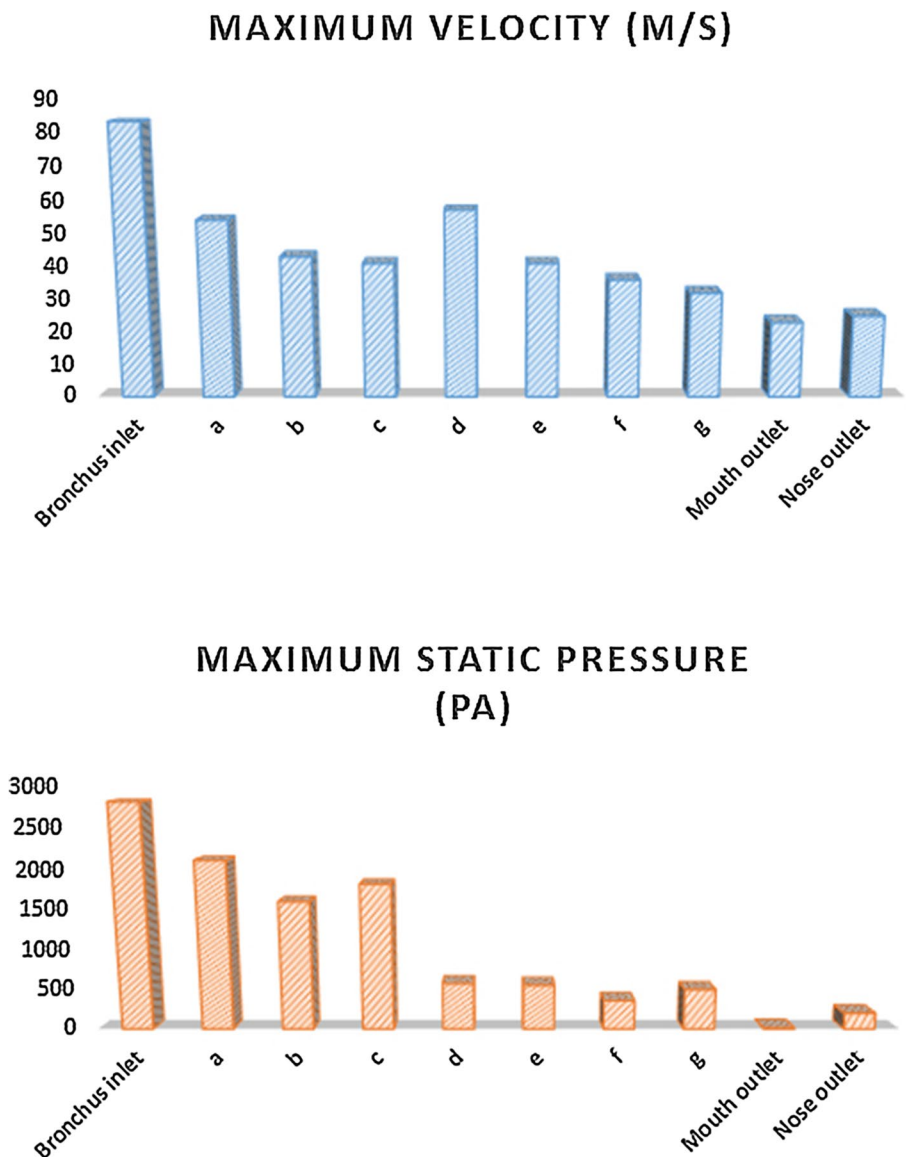


**Table 3** Inlet and outlet flow rates for normal sneeze (case 1)

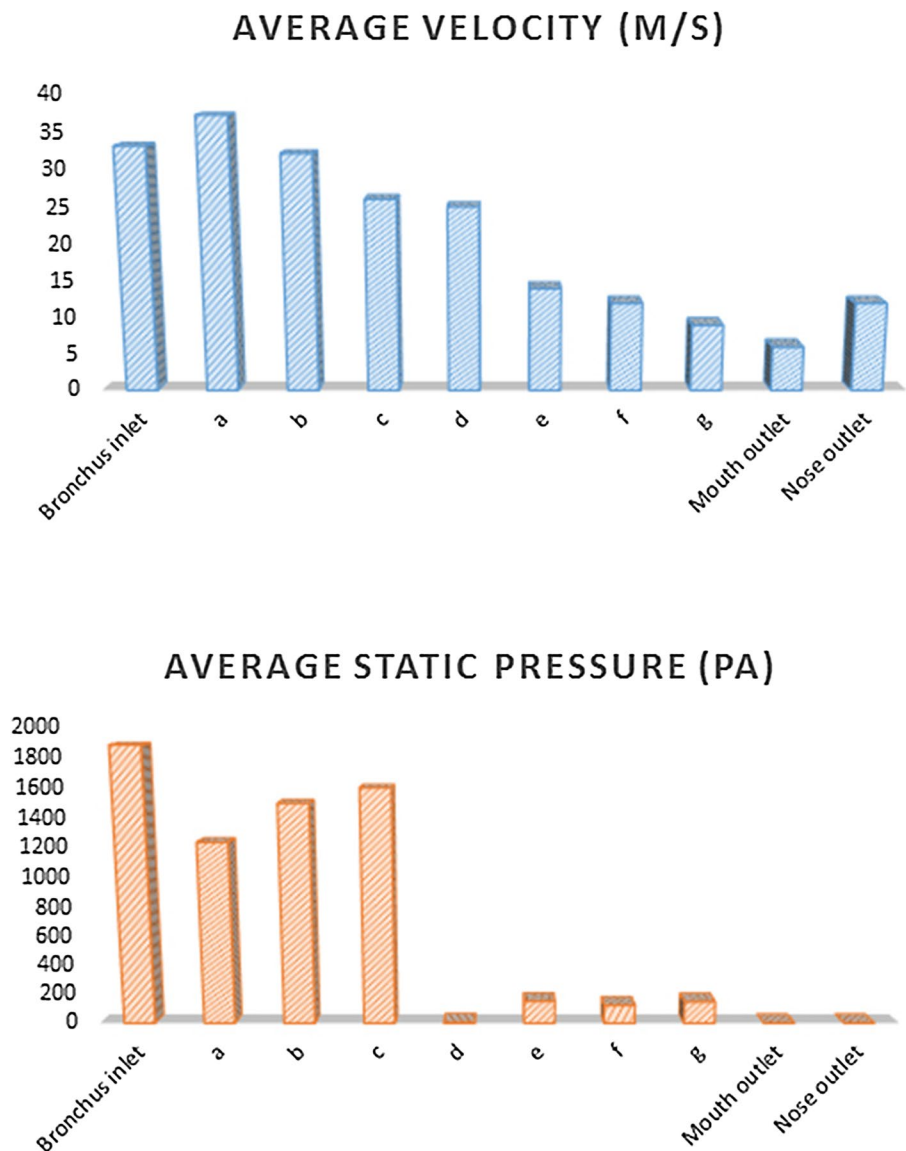
Location	Outlet volume flow rate per inlet volume flow rate of bronchus	Volume flow rate (L/s)
Bronchus	–	7.23
Mouth outlet	68.15%	4.93
Nose outlet	31.85%	2.30

maximum outlet velocity was about 54 m/s, which clearly implies that special attention shall be paid to the particle diffusion during sneezing. Similarly, as it is observed in Fig. 7, the maximum speed is seen in the d cross section. The contour of pressure and velocity distribution in this critical section is shown in Fig. 10; it is obvious that this speed increasing is due to the section geometry conditions.

Table 4 represents inlet and outlet flow rates. Based on the maximum flow rate of the mouth outlet (10.58 L/s), after a trial and error solution, the inlet flow rate of the case was equal to 16.04 L/s, which was 2.2 times greater than the case 1. As seen, the outlet flow rate of nose was 5.42 L/s. Comparing this flow rate to outlet flow rate from the mouth, it was observed that about 34% of the outlet flow rate, during sneezing, exited from the nose and the rest (66%) exited from the mouth. Therefore, it can be concluded that in the second case, the outlet flow rate from the nose has higher percentage.

The average velocity and static pressure at different sections for case 2 are shown in Fig. 11. The maximum average pressure has occurred in the trachea. The maximum average velocity was at section A which also was in trachea. The outlet velocity from the nose was about 2.3 times greater than

**Fig. 8** Average speed and static pressure values at different sections for normal sneeze (case 1)



the outlet velocity from the mouth, which was similar to the first case; the outlet velocity from the nose was greater than the outlet velocity from the mouth.

The deformation contour in the upper airway respiratory system has been shown in Fig. 12. As it can be seen, the most deformation occurred in maxillary sinus and then in thyroid cartilage.

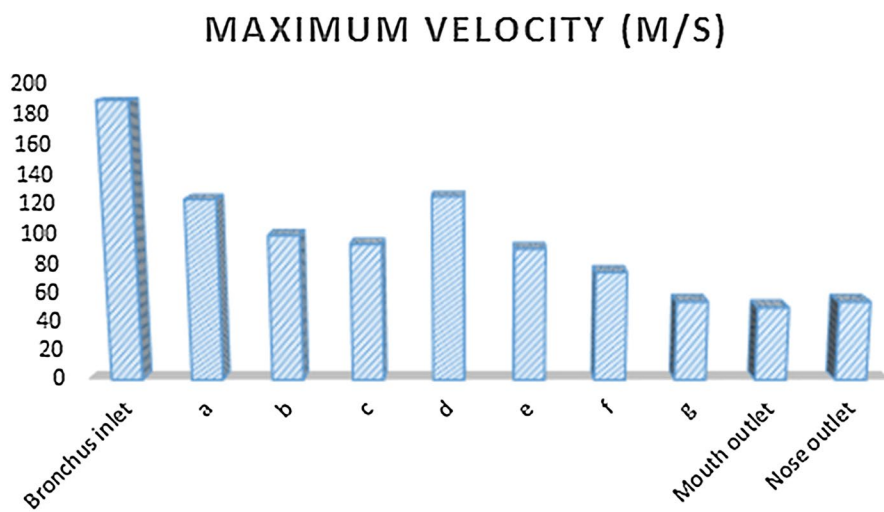
According the last row of Table 5, the rate of the deformation in the thyroid cartilage was increased four times, during closed-mouth sneezing. Actually, the fracture occurred in the thyroid cartilage was the result of this jump as shown in Fig. 13. Also base up on the last column of Table 5, the growth of deformation in the maxillary sinus of the closed-mouth sneezing was less than the growth of deformation in the thyroid cartilage.

## 5 Discussion

In the present study, using FSI method, the sneezing process was simulated in two conditions for a healthy male subject. A completely realistic model was obtained from CT scan images. Using the spirometer, the maximum and average outlet flow rates of the person's mouth were measured while sneezing, which were 4.79 and 10.58 L/s, respectively. These values were applied to the system as a boundary condition for modeling the process. According to the results, during sneezing, taking into account the average outlet flow from the mouth, the velocity of outlet airflow from the mouth and nose reaches 5.5 and 12.1 m/s, respectively. These values were 26.2 and 11.3, respectively, when the maximum flow rate was desired. In both cases, the inlet pressure which occurred in bronchus reached the maximum of 14 kPa. The



**Fig. 9** Maximum static pressure and speed on each section for normal sneeze (case 2)



**MAXIMUM STATIC PRESSURE (PA)**

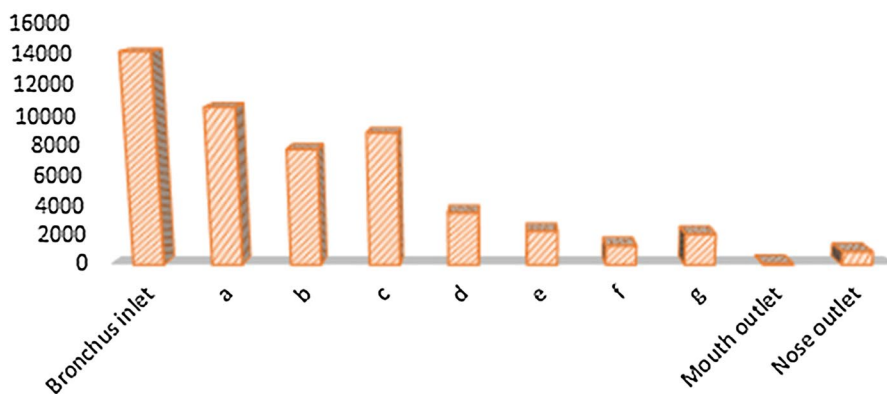


**Fig. 10** Pressure (right) and velocity (left) distribution contours in different sections of the respiratory tract during sneezing for normal sneeze (case 2)

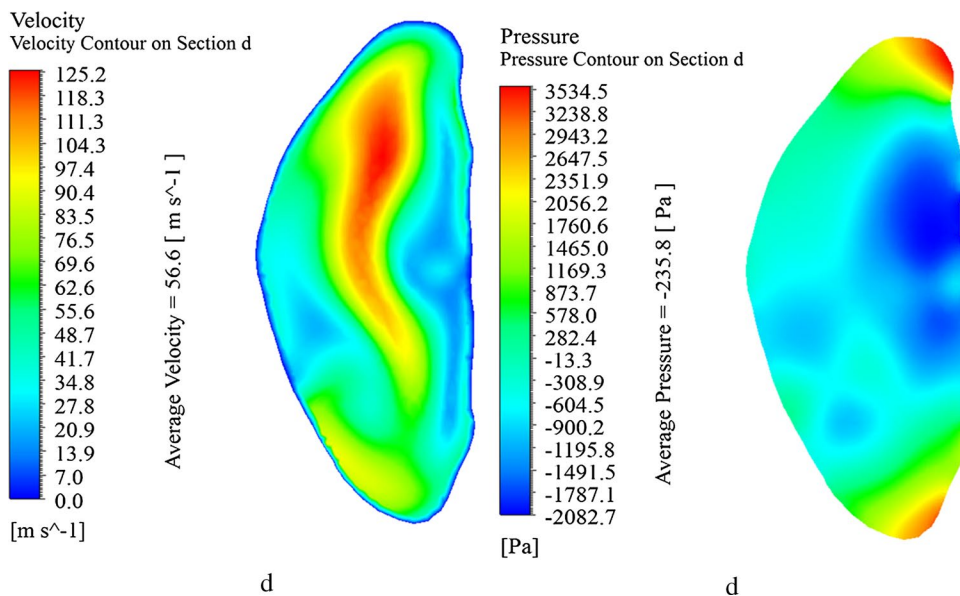


**Table 4** Inlet and Outlet flow rates for normal sneeze (case 2)

Location	Outlet volume flow rate per inlet volume flow rate of bronchus	Volume flow rate(L/s)
Bronchus	–	16.04
Mouth outlet	66.24%	10.62
Nose outlet	33.76%	5.42

average value of this pressure, which is mainly supplied by the diaphragm, was about 2.8 kPa. The maximum flow rate reached 188 m/s, which occurred at trachea inlet. It should be noted that in both simulations, the pressure reached high values in the trachea region which its deformation can be considered in future studies. There is not much literature in the area of simulation of sneezing to be used in validation of our results. In general, Leong et al. [30] have already shown

the potential of CFD method in a systematic overview. The present study confirmed the results by Leong et al. [30] concerning the point that sneezing could be simulated by CFD. In the other words, this technology has improved understanding of the complex nasal anatomy and the implications of disease and surgery on physiology. On the other hand, Rahiminejad et al. [21] showed that during a normal sneeze, the pressure in the trachea reached about 7000 Pa, which was much higher than the pressure level of about 200 Pa during the high activity exhalation. Finally, we found out that during very high airspeeds, due to sneezing, the respiratory regions such as adjacent ethmoid sinuses and the olfactory region are covered by the shock-like expiratory flow which is confirmed by Sommer et al. [31].

According to the results reported by Rahiminejad et al. [21], the pressure boundary condition converged to more real results than the velocity boundary condition at the

**Fig. 11** Average speed and static pressure at different sections for normal sneeze (case 2)

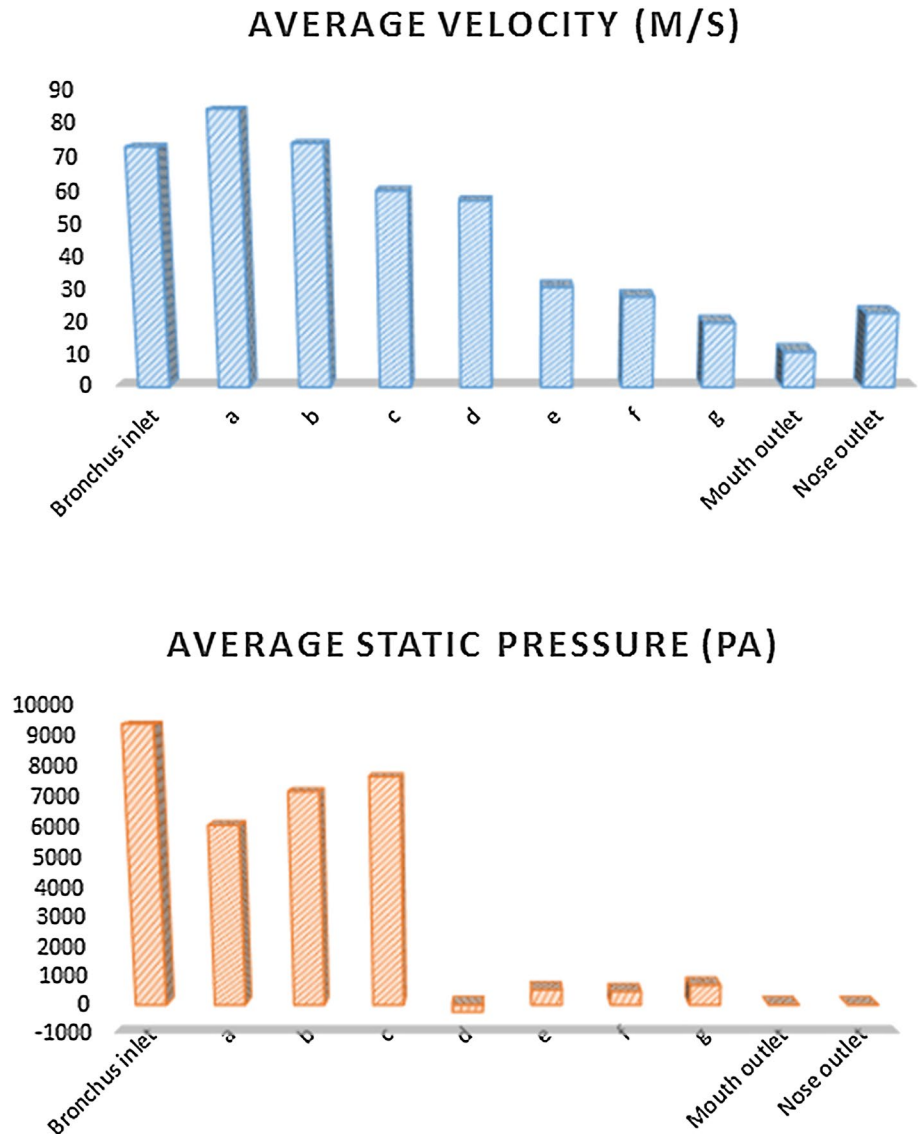


**Fig. 12** Deformation contour in the upper airway respiratory system. (Unit:  $10^2\text{mm}$ ) **a** normal sneeze for case 2. **b** sneeze with closed mouth for case 2

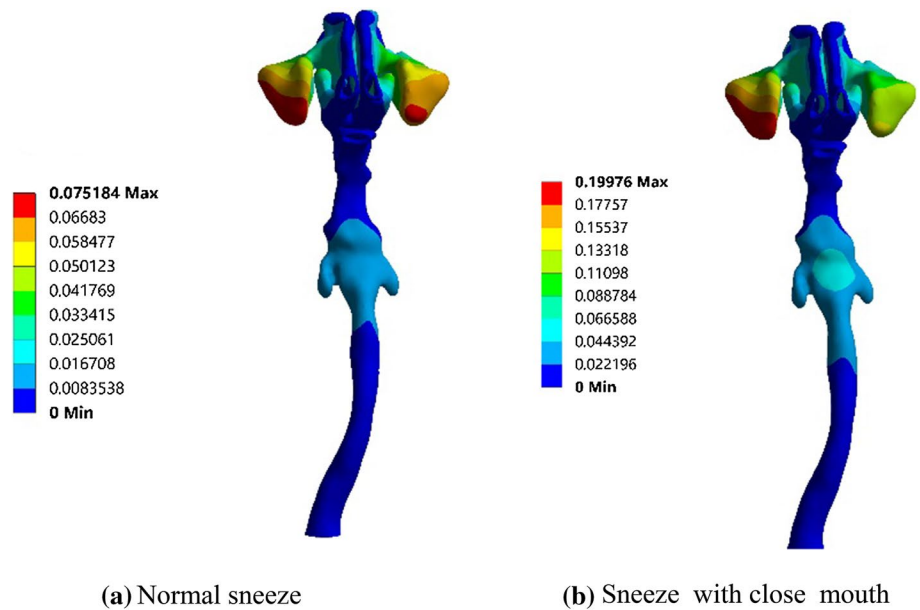


**Table 5** Ratio of the deformation in the thyroid cartilage

Sneeze status for case 2	Deformation (mm)		
	Maxillary	Thyroid cartilage	Ratio maxillary/ thyroid cartilage
A: Normal sneeze	7.52	1.67	4.5
B: Sneeze with close mouth	19.98	6.66	3
Ratio B/A	2.7	4	

input region. Hence, this kind of boundary condition was used at the bronchus inlet. Nunn et al. [32] should be noted that the outlet flow rate of the respiratory system was consistent with the measured maximum outlet flow rate reported in reference. Since the amount of the flow rate during sneezing was not measured experimentally,

Rahiminejad et al. [21] predicted the air flow of sneezing using the maximum exhalation air flow. They considered the approximate average value of the pressure equal to 8 kPa in the trachea entrance for a 24-year-old female and reported the speed and pressure changes in sneezing according to different boundary conditions. In this way, the effect of open and closed mouth and nose during sneezing on the speed and pressure distributions in the human upper airway was attained approximately. In this article, firstly, the experimental results of the mouth volumetric air flow during sneezing were obtained by the spirometer device. According to the results, the average amount of the air flow was equal to 4.79 L/s and its maximum value was 10.58 L/s at the mouth output. The 3D model of the human upper airway is extracted for the same person with CT scan images. Then, by applying the experimental results of

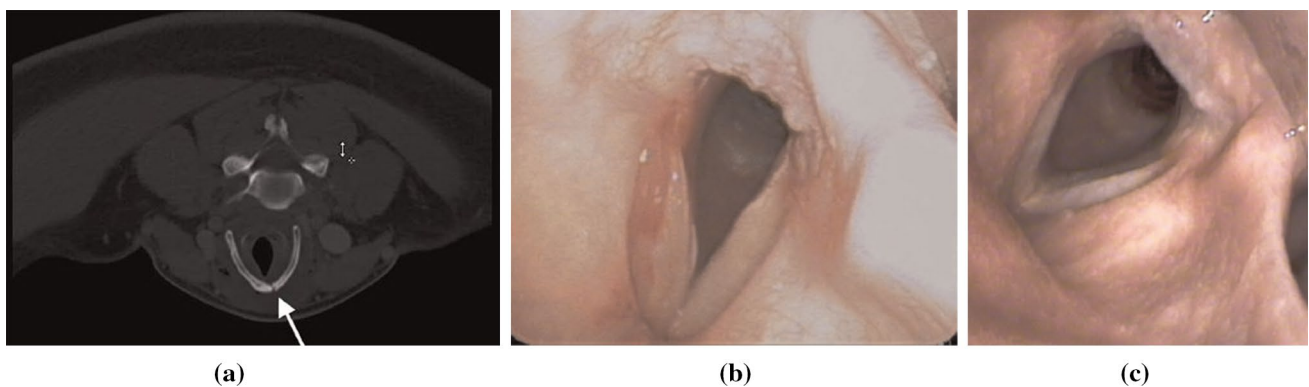


**Fig. 13 a** Axial section of computed tomography scan demonstrating fracture of the thyroid cartilage along the right anterior aspect of the cartilage (arrow). Surrounding emphysema within the cervical fascia

of the neck can also be appreciated. **b** Flexible fiber-optic laryngoscopy examination demonstrating resolving mucosal hemorrhage day of presentation, **c** Two-month follow-up [33]

the airflow as the output boundary condition, the average amount of pressures at the trachea entrance are calculated as 2.8 kPa and 14 kPa for the two cases, respectively (average and a maximum airflow of the mouth outlet). This way, with the help of these real data, the pressure and velocity distributions in normal sneezing were extracted and the results were compared.

According to Table 5, in the mouth-closed sneezing, a fourfold increase in the amount of deformation in the thyroid cartilage was seen compared to the open-mouth sneezing, which occurs suddenly in a fraction of a second. Undoubtedly, because of different levels of individual's tolerance, this leap could damage the thyroid cartilage. As Birch et al. [28] have shown, the value of Young's coefficient is different for each individual person, and therefore, the level of tolerance is different. The correctness of this achievement could be seen in a recent study by Matrka and Li [33] that showed a 35-year-old man's thyroid cartilage was defeated due to closed-mouth sneezing.

## 6 Conclusion

We introduced a model which simulated a normal sneezing for two cases and sneeze with closed mouth for case 2 using experimental data. The results including the velocity and pressure contours of different sections of the airways system were shown. The results showed that the inlet pressure to the tract, existing in the bronchus region, reaches a maximum of 14 kPa. The average value of this pressure, which is mainly supplied by the diaphragm is about 2.8 kPa. We believe that the model should be applied for different persons and an atlas of data could be obtained from different cases. This may help the medical system to have more data about the sneezing process.

Because of Valsalva maneuver during sneezing, the pressure of the pleural cavity pressure is quite high. However, the deformations in the upper airway respiratory system significantly increase due to deformation rate growth in sneezing, and laryngeal fracture can be mentioned as one of the symptoms of this severe deformation during the Valsalva maneuver. The rate of the deformation in the thyroid cartilage was increased four times, during closed-mouth sneezing for case 2. Actually, the fracture occurred in the thyroid cartilage was the result of this jump.

**Acknowledgements** We thank Taba-Parto Shiraz radiology center for assistance with 3D CT scan, and Shamsizadeh clinic that provided the spirometer device that greatly improved the manuscript.

**Funding** The research was not funded by any organization or university.

## Compliance with ethical standards

**Conflict of Interests** The authors of this paper declare that they consider no conflict of interest.

**Human participants** All procedures performed in studies involving human participants were in accordance with the ethical standards of the institutional and/or national research committee and with the 1964 Helsinki declaration and its later amendments or comparable ethical standards.

## References

- Zhang Z, Lessmann R (1996) Computer simulation of the flow field and particle deposition by diffusion in a 3-D human airway bifurcation. *Aerosol Sci Technol* 25:338–352
- Cebral JR, Summers RM (2004) Tracheal and central bronchial aerodynamics using virtual bronchoscopy and computational fluid dynamics. *IEEE Trans Med Imaging* 23(8):1021–1033
- Wen J, Inthavong K, Tu J, Wang S (2008) Numerical simulations for detailed airflow dynamics in a human nasal cavity. *Respir Physiol Neurobiol* 161(2):125–135
- Grgic B, Martin A, Finlay W (2006) The effect of unsteady flow rate increase on in vitro mouth–throat deposition of inhaled boluses. *J Aerosol Sci* 37(10):1222–1233
- Liu Y, So RMC, Zhang CH (2002) Modeling the bifurcation flow in a human lung airway. *J Biomech* 35:465–473
- Moghadas H, Abouali O, Faramarzi A, Ahmadi G (2011) Numerical investigation of nasal septal deviation effect on micro/nano-particles deposition in a human realistic geometry. *Respir Physiol Neurobiol* 177:9–18
- Nithiarasu P, Hassan O, Morgan K, Weatherill NP, Fielder C, Whittet H, Ebdon P, Lewis KR (2008) Steady flow through a realistic human upper airway geometry. *Int J Numer Methods Fluids* 57:631–651
- Tavakoli B, Abouali O, Bagheri MH, Yazdi M, Ahmadi G (2012) Micro particles transport and deposition in realistic geometry of human upper airways. *Int J Eng Trans A (Basics)* 25(4):315–322
- Malve M, Perezdel Palomar A, Lopez-Villalobos JL, Ginel A, Doblare M (2010) FSI analysis of the coughing mechanism in a human trachea. *Ann Biomed Eng* 38:1556–1565
- Chen C, Lin CH, Jiang Z, Chen Q (2014) Simplified models for exhaled airflow from a cough with the mouth covered. *Indoor Air J* 24(6):580–591
- Zhu S, Kato S, Yang JH (2006) Study on transport characteristics of saliva droplets produced by coughing in a calm indoor environment. *Build Environ* 41:1691–1702
- Tang JW, Settles GS (2008) Images in clinical medicine, coughing and aerosols. *New Engl J Med* 15:359
- Gupta J, Lin CH, Chen Q (2009) Flow dynamics and characterization of a cough. *Indoor Air J* 19:517–525
- Wells WF (1955) Airborne contagion and air hygiene: an ecological study of droplet infection. Harvard University Press, Cambridge, pp 1–19
- Xie X, Li Y, Chwang AT, Ho PL, Seto WH (2007) How far droplets can move in indoor environments—revisiting the Wells evaporation-falling curve. *Indoor Air J* 17:211–225
- Jennison MW, Edgerton HE (1940) Droplet infection of air; high-speed photography of droplet production by sneezing. *Proc Soc Exp Biol Med* 43:455–458
- Tang JW, Nicolle AD, Klettner CA, Pantelic J, Wang L, Suhaimi AB, Tan AYL, Ong GWX, Su R, Sekhar C, Cheong DDW, Tham KW (2013) Airflow dynamics of human jets: sneezing and

- breathing—potential sources of infectious aerosols. *Plos ONE J* 8(4):e59970. <https://doi.org/10.1371/journal.pone.0059970>
18. Nishimura H, Sakata S, Kaga A (2013) A new methodology for studying dynamics of aerosol particles in sneeze and cough using a digital high-vision, high-speed video system and vector analyses. *Plos ONE J* 8(11):e80244. <https://doi.org/10.1371/journal.pone.0080244>
  19. Bourouiba L, Dehandschoewercker E, Bush JWM (2014) Violent expiratory events: on coughing and sneezing. *J Fluid Mech* 745:537–563
  20. Gwaltney JM, Hendley JO, Phillips CD, Bass CR, Mygind N, Winther B (2000) Nose blowing propels nasal fluid into the paranasal sinuses. *Clin Infect Dis* 30(2):387–391
  21. Rahiminejad M, Haghighi A, Dastan A, Abouali O, Farid M, Ahmadi G (2016) Computer simulations of pressure and velocity fields in a human upper airway during sneezing. *Comput Biol Med* 71:115–127
  22. Faden DL, Elackatuu A, Platt M (2011) The closed-airway sneeze: an unusual cause of laryngeal fracture. *J Otolaryngol Head Neck Surg* 145(3):515–516
  23. Martinez BA, Juara AM, Moya LJJ (2007) Fracture of thyroid cartilage after a sneezing episode. *Acta Otorrinolaringol Esp* 58(2):73–74
  24. Mylavaram G, Murugappan S, Mihaescu M, Kalra M, Khosla S, Gutmark E (2009) Validation of computational fluid dynamics methodology used for human upper airway flow simulations. *J Biomech* 42:1553–1559
  25. Zubair M, Abdullah MZ, Ismail R, Shuaib IL, Hamid SA, Ahmad KA (2012) Review: a critical overview of limitations of CFD modeling in nasal airflow. *J Med Biol Eng* 32(2):77–84
  26. MIR MiniSpir™. Simplified operation guide
  27. Zhao M, Barber T, Cistulli PT, Sutherland K, Rosengarten G (2013) Simulation of upper airway occlusion without and with mandibular advancement in obstructive sleep apnea using fluid-structure interaction. *J Biomech* 46:2586–2592
  28. Birch MJ, Srodon PD (2009) Biomechanical properties of the human soft palate. *Cleft Palate Craniofac J* 46(3):268–274
  29. Patankar S (1980) Numerical heat transfer and fluid flow. Series on computational methods in mechanics and thermal science hemisphere publishing corporation, 1st edn. CRC Press, Boca Raton. <https://doi.org/10.1201/9781482234213>
  30. Leong SC, Chen XB, Lee HP (2010) A review of the implications of computational fluid dynamic studies on nasal airflow and physiology. *Rhinology* 48:139–145
  31. Sommer F, Scheithauer M, Kröger R, Rettinger G, Lindemann J (2014) Sneezing as a mechanical defence—a numerical simulation and analysis of the nasal flow. *Laryngo- Rhin- Otologie* 93(11):746–750
  32. Nunn AJ, Gregg I (1989) New regression equations for predicting peak expiratory flow in adults. *BMJ* 298:1068–1070
  33. Matrka L, Li M (2018) Laryngeal fracture following violent sneeze: management and biomechanical analysis. *Am Acad Otolaryngol Head Neck Surg* 2:24

**Publisher's Note** Springer Nature remains neutral with regard to jurisdictional claims in published maps and institutional affiliations.